Journal of Computational Methods in Molecular Design, *2017, 7 (1):38-50*

ISSN : 2231- 3176
CODEN (USA): JCMMD

Experimental and Computational Study of the Azo Dye Derived From 4-Amino-1,2,4-Triazole and Its Metal Complexes

SN Chaulia*

Department of Chemistry, G. M. University, Sambalpur, Odisha, India
Corresponding Email: satyanarayanchaulia@gmail.com

ABSTRACT

Metal complexes of Co(II), Ni(II), Cu(II) and Zn(II) of the azo dye ligand derived from 4-amino-1,2,4-triazole and 5-sulphosalicylic acid have been synthesised. These complexes and the ligand have been characterised spectroscopically with the help of IR, NMR and electronic spectra. Theoretical study of the ligand and its metal complexes has been made in order to determine their stability, geometrical and electronic properties. Global reactive descriptors of the investigating compounds such as electrochemical potential, chemical hardness, electrophilicity index are calculated from the HOMO and LUMO of the ligand and metal complexes. The experimental IR and electronic spectral data are compared with the computationally generated data. The QSAR properties of the ligand and complex compound are generated to predict their biological activities.

Keywords: Electrochemical potential, QSAR properties, lipophilicity, Biological activities

INTRODUCTION

Azo compounds derived from Heterocyclic moieties are attracting the attention of the scientific communities in recent years due to their application for colouring textiles, rubbers and plastics [1], these compounds can be used in the field of pharmaceutical as antibacterial, antifungal, antiviral [2]. Azo dyes derived from thiophene, pyrrole and azoles have been used for electronic applications such as optical switching, second harmonic generation and organic sensitised solar cells [3]. The use of azo dyes derived from heterocyclic amines as colorimetric sensors, in non-linear optical devices, liquid crystalline display and sensitizers [4] has been reported in recent years. It has also been reported that the activity of the azo group increases when it is attached with heterocyclic rings [5]. With a view of this, the synthesis of the ligand derived from 4-amino-1,2,4-triazole and its metal complexes, characterisation and computational study are presented.

EXPERIMENTAL

Materials and methods

All the solvents, the metal salts and other chemicals used are of either analytical grade or high purity supplied by Merck and BDH. Elemental analysis of the ligand and complexes is carried out by Perkin–Elmer elemental analyser, cobalt, nickel, copper contents is determined by Perkin–Elmer2380 atomic absorption spectroscopy and chloride contents is estimated by standard procedure.

Magnetic susceptibility of the complexes is measured by Guoy's balance using $Hg[Co(NCS)_4]$ as a calibrant at room temperature and diamagnetic correction have been made by pascal's constants, IR spectra of the ligand and metal complexes are recorded on using KBr pellets by perkin elmer FT-IR spectrometer within the range 4000-450 cm^{-1}, UV-Visible spectra of the complexes are collected using a THERMO SPECTRONIC 6 HEXIOS α,^1H NMR spectra of the ligand and the Zn(II) complex are obtained from Bruker AV III 500 MHZ FT NMR spectrometer using TMS as reference.

Computational strategy

In this work calculations were performed by employing quantum chemical approach with Becke three parameter hybrid method [6] using the Lee-Yang-Par correlation functional [7] with the 3-21G(d, p) basis set.

Synthesis of the ligand

The ligand was synthesized by the coupling reaction between the diazonium chloride derived from 4-amino-1,2,4-triazole and 5-sulphosaicylic acid. The diazonium chloride was prepared by dissolving 0.84 g of 0.01 M of 4-amino-1,2,4-triazole in hydrochloric acid, cooling it to 0-5℃ and adding equivalent amount of ice–cooled sodium nitrite solution with vigorous stirring. The diazonium chloride was then added to 0.01 M of 2.18 g of 5-sulphosaicylic acid. The coloured azo compound was filtered, dried in vacuum and recrystallised from ethanol. Thin layer chromatography technique was adopted to collect pure azo compound (Figure 1).

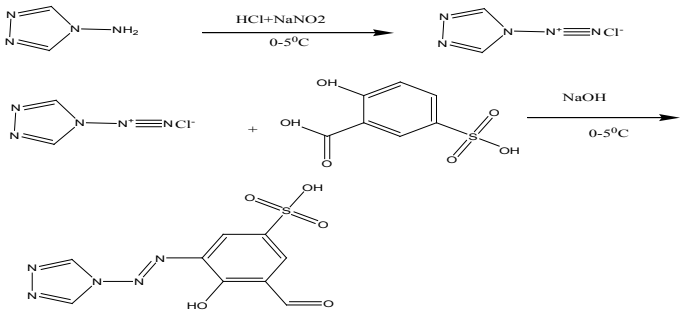

Figure 1: Synthesis of the ligand

Synthesis of the metal complexes

The ethanol solution of each of the Co(II), Ni(II), Cu(II) and Zn(II) chloride was mixed with the solution of the ligand in DMF separately and refluxed for 1 h at a temperature of 60℃. The refluxed solution was cooled and added with concentrated ammonium chloride drop by drop to get the neutral reaction mixture. The reaction mixture was filtered, dried in vaccum and recrystallised from the DMF solution. This procedure was repeated to get the metal complexes of Co(II), Ni(II), Cu(II) and Zn(II) complexes (Figure 2 and Figure 3).

$$2\,MCl_2 + LH \xrightarrow[NH_4OH]{\text{Reflux 1 hour, } 60^0C} [M_2LCl_3H_2O)_5] + NH_4Cl$$

M= Co(II), Ni(II),Cu(II)

$$2\,MCl_2 + LH_2 \xrightarrow[NH_4OH]{\text{Reflux 1 hour, } 60^0C} [M_2LCl_3(H_2O)] + NH_4Cl$$

M= Zn(II)

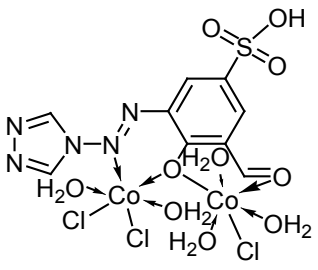

Figure 2: Structure of Co(II) complex

RESULTS

Element Analysis data of the ligand and its metal complexes are provided in the Table 1 which indicates the formula of the compound complexes as M2L, where M represents Co(II), Ni(II), Cu(II) and Zn(II) and L is the deprotonated azo ligand.

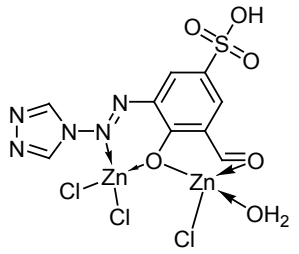

Figure 3: Structure of Zn(II) complex

Table 1: Analytical data

Comp	Colour	Yield(%)	M.P (°C)	% Found(calcd)				
				M	C	H	N	Cl
LH	Reddish brown	68	65	-	36.12 (36.37)	2.05 (2.37)	23.24 (23.56)	-
$[Co_2LCl_3(H_2O)_5]$	Red	48	>300	19.29 (19.31)	17.67 (17.70)	2.52 (2.64)	11.41 (11.48)	17.37 (17.42)
$[Ni_2LCl_3(H_2O)_5]$	Coffee red	46	>300	19.18 (19.24)	17.63 (17.72)	2.54 (2.64)	11.39 (11.47)	17.42 (17.43)
$[Cu_2LCl_3(H_2O)_5]$	Light green	52	>300	20.48 (20.51)	17.40 (17.44)	2.56 (2.60)	11.26 (11.30)	16.98 (17.16)
$[Zn_2LCl_3(H_2O)]$	Brick red	45	>300	24.98 (25.22)	19.35 (19.60)	1.41 (1.46)	12.48 (12.70)	18.95 (19.29)

IR spectra and mode of bonding

The IR spectrum of the ligand and its metal complexes (Table 2 and Figures 4-9) are compared to ascertain the mode of bonding between the ligand and the metal ions. The IR spectrum of the ligand reveals a broad band at 3901 cm^{-1} which is missing in all metal complexes. Further, the spectrum of the ligand shows a high intensity band at 1294 cm^{-1} due to vibration of C-O group which is shifted to medium intensity band that is at ~1340 cm^{-1} in metal complexes that suggests deprotonation of the phenolic -OH and formation of bond between the metal ions and the oxygen atoms of the phenolic -OH [8]. The band observed at 1474 cm^{-1} in the IR spectrum of the ligand is due to the vibration of azo group but this band is shifted to lower frequency in the metal complexes at ~1468 cm^{-1} that indicating the coordination of the azo nitrogen with the metal ions [9]. A strong band is also seen in the spectrum of the ligand at 1624 cm^{-1} which is shifted to ~1620 cm^{-1} in the spectra of the metal complexes that suggests the bonding of carbonyl oxygen with the metal ions [10]. The spectra of complexes reveal the presence of band at ~3350 cm^{-1} due to the vibration frequency of O-H of coordinated. The presence of coordinated water is further confirmed by the rocking band at ~899 cm^{-1} and twisting band at ~795 cm^{-1} [11]. Two new bands also appeared in the metal complexes in the low frequency range of ~570 cm^{-1} and ~441 cm^{-1} which may be assigned to the vibration of (M-N) and (M-O) that indicates participation of azo nitrogen and oxygen of phenolic group with the metal ions through coordinate bond [12]. The Figure 7 and Figure 8 indicate comparison between experimental and computational data.

Table 2: IR data of the ligand and its metal complexes

Sl no	ν(C-O)/cm^{-1} Expt/Calcd	ν(N=N)/cm^{-1} Expt/Calcd	ν(C=O)/cm^{-1} Expt/Calcd	ν(M-N)/cm^{-1} Expt/Calcd	ν(M-O)/cm^{-1} Expt/Calcd
Ligand	1294/1320	1474/1468	1624/1620	-	-
$[Co_2LCl_3(H_2O)_5]$	1340/1342	1470/1475	1621/1616	569/565	424/426
$[Ni_2LCl_3(H_2O)_5]$	1329/1332	1468/1478	1610/1603	571/566	439/440
$[Cu_2LCl_3(H_2O)_5]$	1336/1351	1467/1482	1622/1626	570/572	441/443
$[Zn_2LCl_3(H_2O)]$	1318/1324	1461/1466	1620/1654	563/559	435/433

NMR spectra

The NMR spectra of the ligand and its Zn(II) complex is recorded in DMF solution in order to characterize the ligand and ascertain the mode of bonding between the ligand and the metal ions. The NMR spectrum of the ligand (Figure 10) shows a multiplet at δ 5.8-8.11 ppm indicating the presence of aromatic protons. The presence of aromatic hydroxyl proton is confirmed by a peak at δ10.12 ppm. The spectrum of the ligand also gives a peak at δ12.73 ppm due to the presence of aldehydic proton.

The spectrum of the Zn (II) complex shows all peaks as given by the ligand except the peak due to the proton of the hydroxyl group. This observation indicates deprotonation of the phenolic (–OH) and the oxygen atom coordinates with the metal ion. This fact is also supported by the IR data (Figure 11).

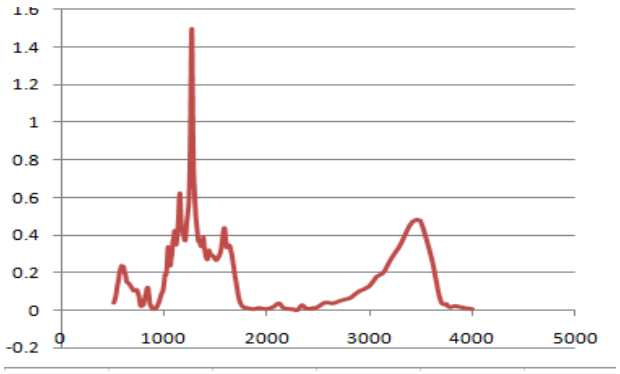

Figure 4: IR spectrum, experimental (Ligand)

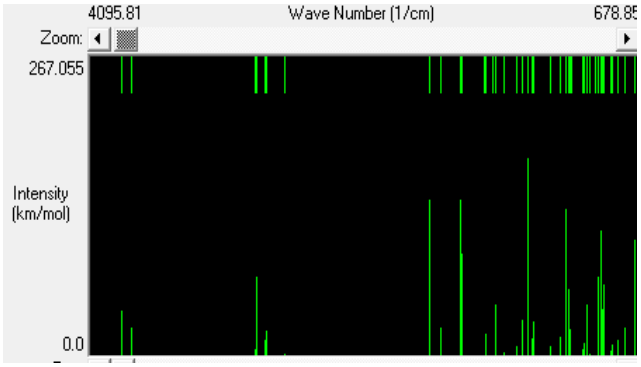

Figure 5: IR spectrum, computed (Ligand)

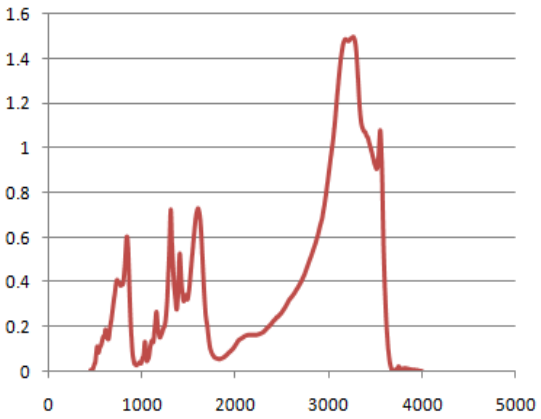

Figure 6: IR spectrum, experimental (Co(II) complex)

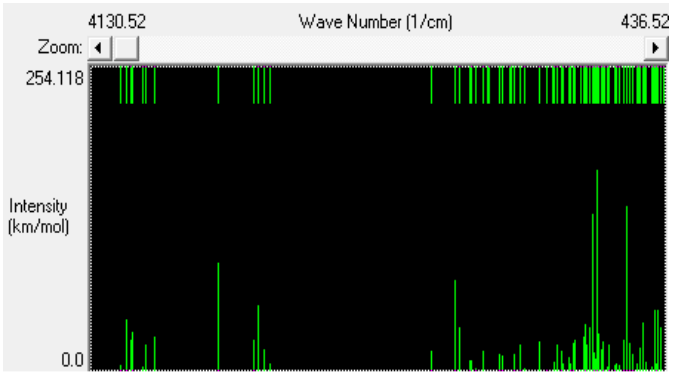

Figure 7: IR spectrum, computed (Co(II) complex)

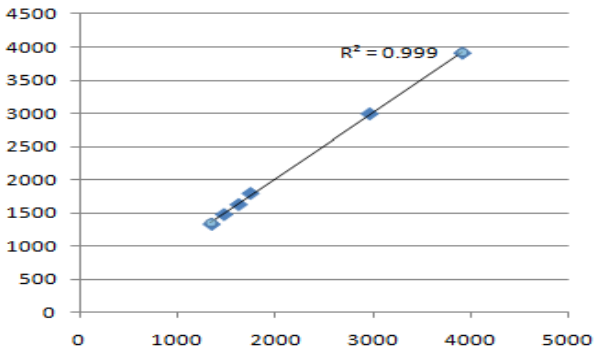

Figure 8: IR spectrum, experimental (Ligand)

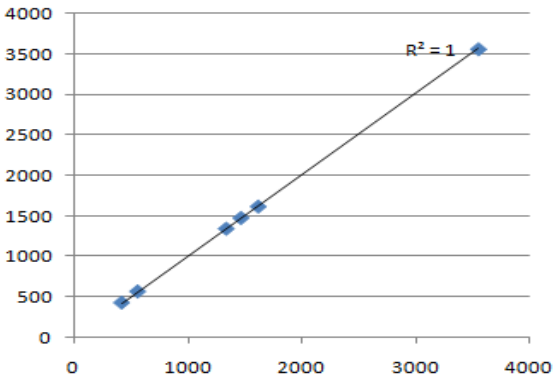

Figure 9: Experimental verses calculated frequency of Co(II) complex

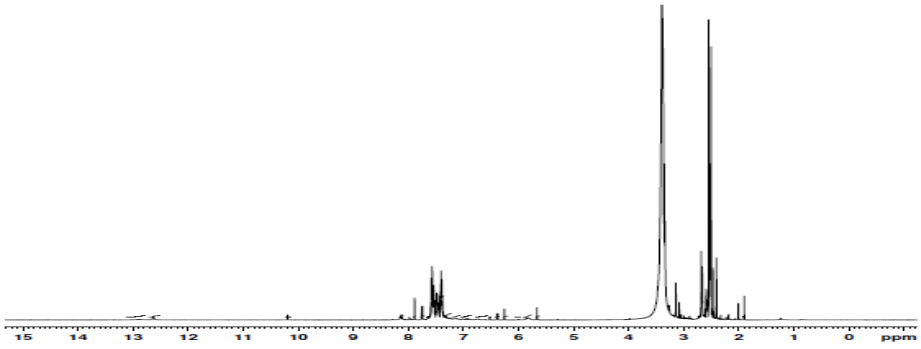

Figure 10: Experimental NMR spectrum of the ligand

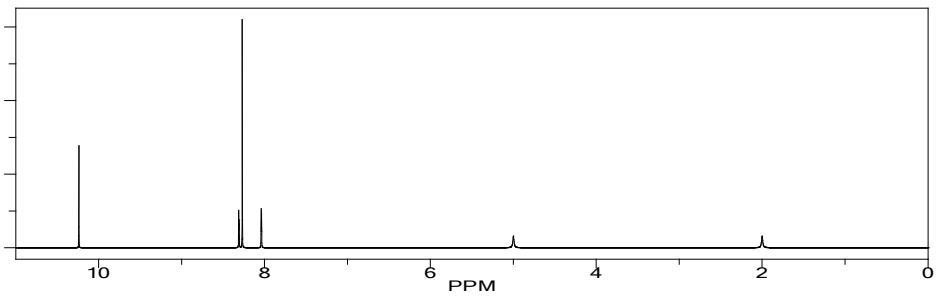

Figure 11: Calculated NMR spectrum of the ligand

Electronic spectra

The electronic spectra of the ligand and its metal complexes (Table 3 and Table 4 and Figures 12-14) were recorded and their magnetic measurement was taken to establish the geometric structures of the complexes. The experimental

spectral data are compared with the calculated data generated by the computation process and both data are in good agreement.

Table 3: Experimental and computed wavelength of the ligand and its metal complexes

Compound	Expt wavelength (nm)	Calcd wavelength (nm)	Assignment
Ligand	311 251, 245	305 254,249	n-π * π-π *
$[Co_2LCl_3(H_2O)_5]$	1230 810 730 580 350	1223 801 722 583 377	$^4T_{1g}(F) \rightarrow {}^4T_{2g}(F)$ $^4T_{1g}(F) \rightarrow {}^4A_{2g}(F)$ $^4T_{1g}(F) \rightarrow {}^4T_{2g}(P)$ CT
$[Ni_2LCl_3(H_2O)_5]$	780 560 460 280	783 568 468 282	$^3A_{2g}(F) \rightarrow {}^3T_{2g}(F)$ $^3A_{2g}(F) \rightarrow {}^3T_{1g}(F)$ $^3A_{2g}(F) \rightarrow {}^3T_{1g}(P)$ CT
$[Cu_2LCl_3(H_2O)_5]$	610 280	597 281	$^2E_g \rightarrow {}^2T_{2g}$

Table 4: Electronic parameters of the complexes

Compound	B	β_{35}	% of β_{35}	υ_2/υ_1	Geometry	μ_{eff} B.M.
$[Co_2LCl_3(H_2O)_5]$	340.4	0.350	65	1.51	Distorted octahedral	3.67
$[Ni_2LCl_3(H_2O)_5]$	142.4	0.136	86.4	1.39	Distorted octahedral	2.51
$[Cu_2LCl_3(H_2O)_5]$	-	-	-	-	Distorted octahedral	1.58

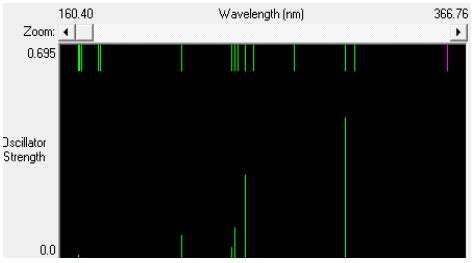

Figure 12: Electronic spectrum of the ligand (Calcd)

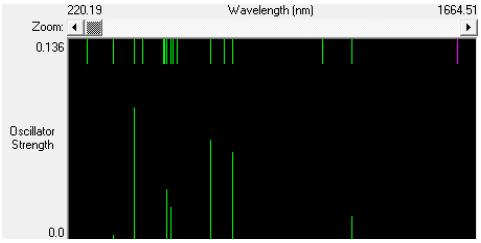

Figure 13: Electronic spectrum of the Co(II) complex (Calcd)

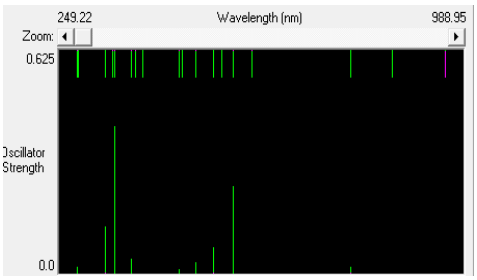

Figure 14: Electronic spectrum of the Ni(II) complex (Calcd)

The ligand shows three bands at 305 nm (32786 cm-1), 254 nm (39370) and 249 nm (40160) due to n-π * and π-π * transitions.

The electronic spectrum of Co(II) complex (Table 3) exhibits four bands at 8130, 12345 and 17152 cm^{-1} assignable to $^4T_{1g}(F) \rightarrow {}^4T_{2g}(F)(\nu_1)$, $^4T_{1g}(F) \rightarrow {}^4A_{2g}(F)(\nu_2)$, $^4T_{1g}(F) \rightarrow {}^4T_{2g}(P)(\nu_3)$ transitions which are characteristic of octahedral geometry [13].The fourth band is a CT band and the electronic parameters such as Dq, B, β, υ_2/υ_1 and % σ are calculated by using following equations and given in the Table 4.

$$Dq=\nu_2-\nu_1/10 \quad (1)$$

$$B=\nu_2+\nu_3-3\ \nu_1/15 \quad (2)$$

$$\beta_{35}=B/971 \quad (3)$$

$$\beta_{35}\%=(1-\beta) \times 100 \quad (4)$$

Similarly, the Ni(II) complex(2) (Graph 3) also exhibits three d-d transition three bands at 12820, 17857, 21739 cm^{-1} corresponding to $^3A_{2g}(F) \rightarrow {}^3T_{2g}(F)$, $^3A_{2g}(F) \rightarrow {}^3T_{1g}(F)$, $^3A_{2g}(F) \rightarrow {}^3T_{1g}(P)$ transitions, these suggests octahedral geometry for the Ni(II) complex [14]. The fourth band is a CT band and parameters like Dq, B, β, υ_2/υ_1 and % β_{35} are calculated by using following equations:

$$Dq=\nu1/10 \quad (5)$$

$$B=\nu_2+\nu_3-3\ \nu_1/15 \quad (6)$$

$$\beta_{35}=B/1041 \quad (7)$$

$$\beta_{35}\%=(1-\beta_{35}) \times 100 \quad (8)$$

The experimental spectral data of the ligand and its metal complexes are compared with the computationally generated Electronic spectral data of the same investigating compounds. The data in the table indicate that the experimental data are in good agreement with the calculated data which is supported by the correlation coefficient (Figure 15).

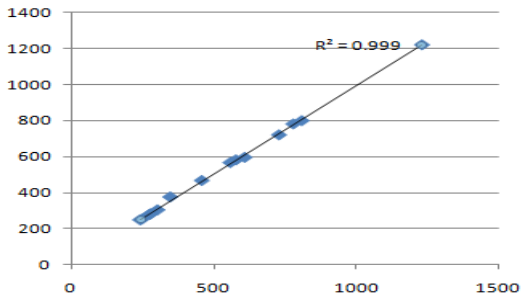

Figure 15: Experimental verses calculated wavelength of the complexes

The Racah parameter (B) of the Co(II) and Ni(II) complexes are found to be less than the free ion values and Nephelauxetic (β35) parameter for both the complexes is less than one. All these observations suggest that the metal ligand bonds in the complexes are covalent in nature.

The spectrum of Cu(II) complex shows a CT bands at 35714 cm^{-1} and one d-d transitions band at 16393 cm^{-1} which may be assigned to $^2E_g \rightarrow {}^2T_{2g}$ transition supporting a distorted octahedral configuration for the complex [15].

The magnetic moment of the Co(II), Ni(II) and Cu(II) complexes are found to be 3.67 B.M., 2.51 B.M. and 1.58 B.M., respectively. All these values indicate octahedral geometry for the metal complexes [16]. The Zn(II) complex is found to be diamagnetic, hence tetrahedral geometry is suggested from the analytical and magnetic data.

Computational study

The structures of all the studied compounds are drawn and optimised. Frequency calculations have been performed to verify the nature of the optimised geometry. The absence of imaginary value in the wave numbers indicates successful geometry optimisation.

Electrostatic potential map

The electrostatic potential map (MEP, Figure 16) indicates the relative sites for electrophilic and nucleophilic attack with respect to biological and hydrogen bonding interactions. It also provides information relating to charge distribution of the molecule [17]. The bio-reactivity of a molecule can be determined by identifying possible sites of the electrostatic interaction between reacting molecules. So the MEP is calculated by using the B3LYP method. The red and blue colour in MEP of the molecule reflects the most reactive sites of electrophilic and nucleophilic attack respectively. It is seen from the MEP that negative regions (red) are mainly localized over the O-atoms of the hydroxyl group, O-atom of the carbonyl group and N-atom of the azo group, so the metal ions are coordinating to the ligand through the azo Nitrogen atom, hydroxyl oxygen atom and carbonyl oxygen atom (Table 5).

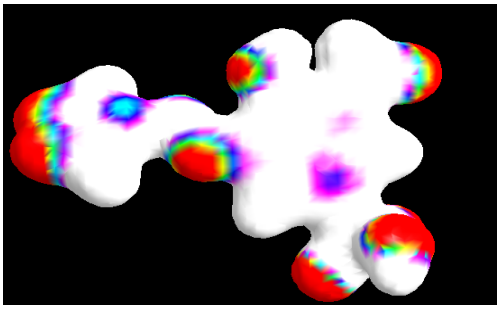

Figure16: Electrostatic potential of the ligand

Table 5: Selected bond length of the metal complexes

Compound	N(6)-Co(21)-O(20)	O(20)-Co(21)-Cl(25)	O(27)-Co(21)-Cl(24)	Geometry
$[Co_2LCl_3(H_2O)_5]$	95.119°	84.879°	89.928°	Distorted octahedral
$[Ni_2LCl_3(H_2O)_5]$	99.344°	112.09°	84.504°	Distorted octahedral
$[Cu_2LCl_3(H_2O)_5]$	102.411°	113.576°	76.126	Distorted octahedral
$[Zn_2LCl_3(H_2O)]$	64.142	97.968	111.860	Distorted tetrahedral

Global reactive descriptors

Reactive descriptors such as Hardness, Electrochemical Potential, Electrophilicity can be calculated from the frontier molecular orbitals such as HOMO and LUMO. Conceptual DFT defines chemical potential μ as the first derivative of energy with respect to number of electrons.

$$\mu = \left(\frac{\partial E}{\partial N}\right)\vartheta(\mathrm{r}) \tag{9}$$

where E=energy, N=number of electrons of the system at constant external pressure ϑ(r).

and chemical hardness n as the half of the second derivative of energy with respect to number of electrons, so chemical hardness will the first derivative of energy with respect to number of electrons.

$$n = \frac{1}{2}\left(\frac{\partial \mu}{\partial N}\right)\vartheta(\mathrm{r}) \tag{10}$$

But chemical potential (μ) and chemical hardness (n) are also calculated in most cases in terms ionisation potential (IP) and electron affinity(EA) and therefore,

$$\mu = -\left(\frac{IP + EA}{2}\right) \tag{11}$$

and

$$n = \left(\frac{IP - EA}{2} \right) \tag{12}$$

and the electronegativity is defined as the negative of the chemical potential according to DFT.

Parr and co-workers proposed electrophilicity index [18,19] as a measure of stabilisation in energy when the system acquires additional energy from the environment and it contains information about both electron transfer and stability. The electrophilicity of a compound can be represented as

$$\omega = \left(\frac{\mu 2}{2n} \right) \tag{13}$$

DISCUSSION

The analytical data indicates that theoretical values are in good agreement with the experimental values.

The experimental data of the ligand and its metal complexes are compared with the computationally generated IR data of the same investigating compounds. The data in the table indicate that the experimental data are in good agreement with the calculated data which is supported by the correlation coefficient. The NMR and electronic spectra also confirms bonding between the metal ion and donor atoms of the ligand (Figures 17-29).

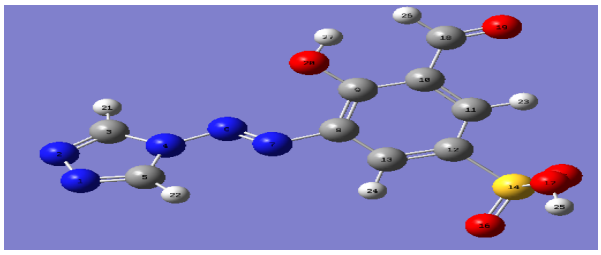

Figure 17: Optimised geometry of the ligand

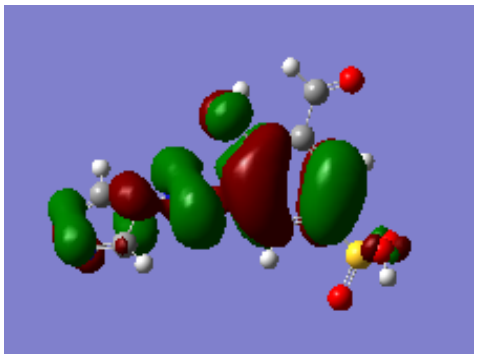

Figure 18: HOMO of the ligand

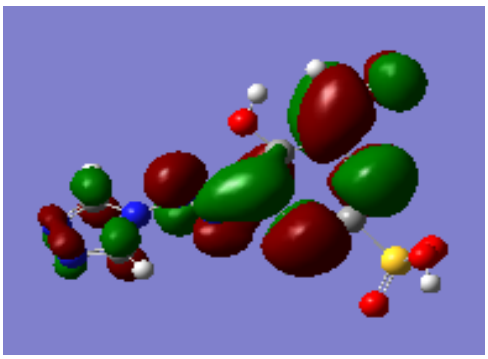

Figure 19: LUMO of the ligand

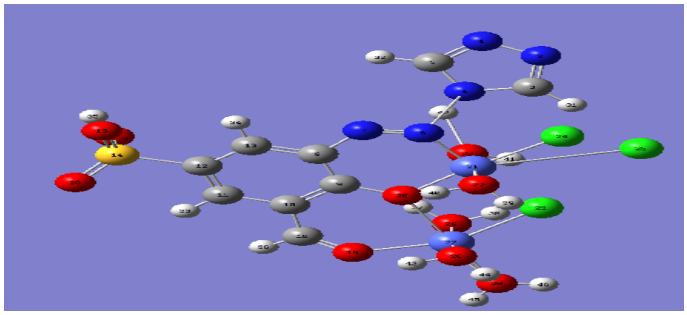

Figure 20: Optimised geometry of the Co(II) complex

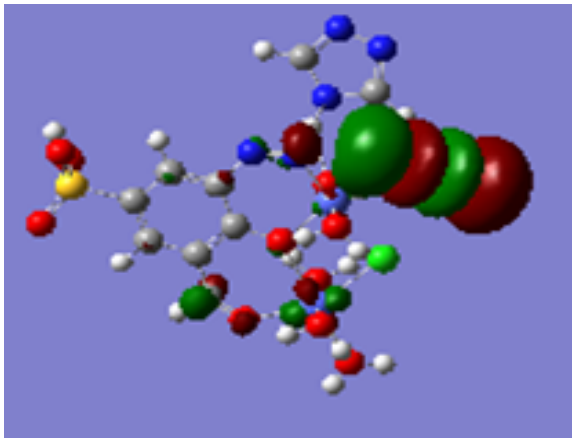

Figure 21: HOMO of the Co(II) complex

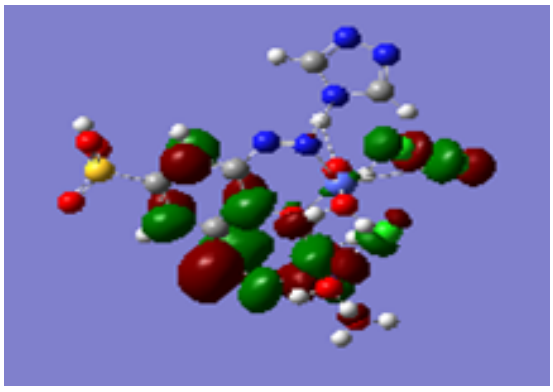

Figure 22: LUMO of the Co(II) complex

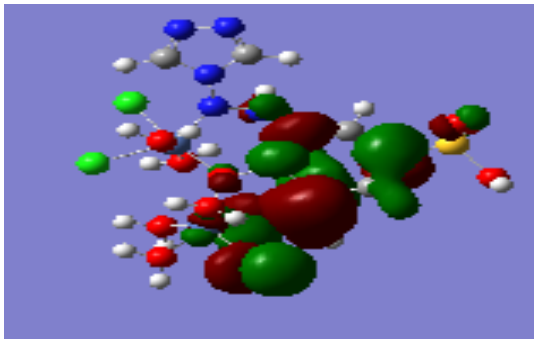

Figure 23: HOMO of the Ni(II) complex

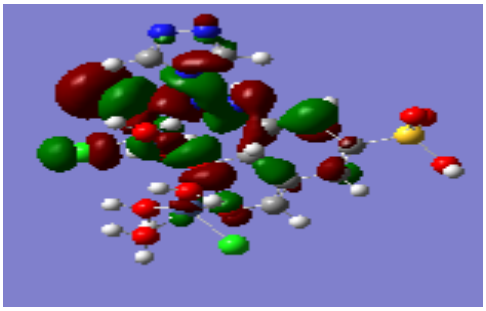

Figure 24: LUMO of the Ni(II) complex

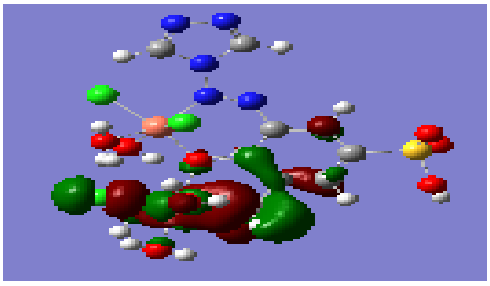

Figure 25: HOMO of the Cu(II) complex

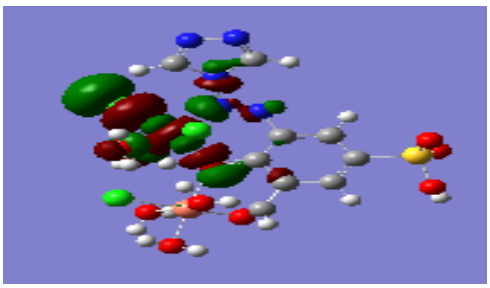

Figure 26: LUMO of the Cu(II) complex

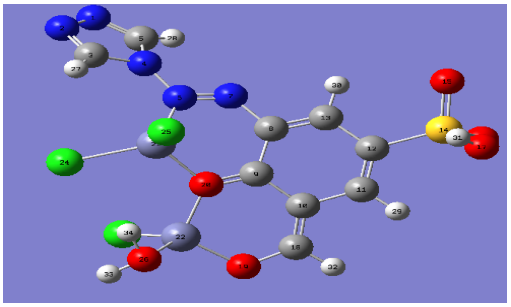

Figure 27: Optimised geometry of the Zn(II) complex

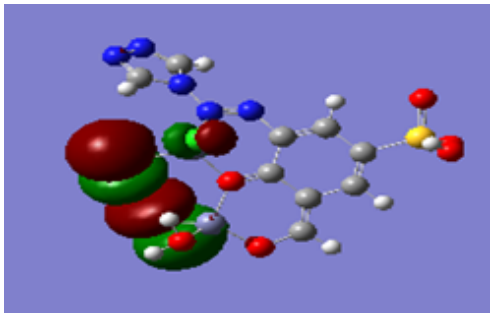

Figure 28: HOMO of the Zn(II) complex

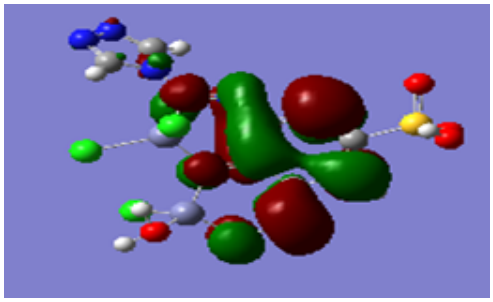

Figure 29: LUMO of the Zn(II) complex

The global reactive descriptors of the ligand and its metal complexes are calculated and summarized in the Table 6. It is seen from the table that metal complexes are more reactive than the ligand and the reactivity of the complexes follows the following order:

Table 6: Global reactive descriptors

Compound	HOMO/eV	LUMO/eV	η/eV	μ/eV	ω
Ligand	-8.4928	0.5010	4.4969	-3.9959	1.7753
$[Co_2LCl_3(H_2O)_5]$	-4.5571	-0.9954	1.7808	-2.7762	2.1639
$[Ni_2LCl_3(H_2O)_5]$	-6.2177	-1.5588	1.8294	-3.8882	3.2451
$[Cu_2LCl_3(H_2O)_5]$	-7.0774	-1.4484	2.3846	-4.2629	3.8103
$[Zn_2LCl_3(H_2O)]$	-8.7610	-1.4435	3.6587	-5.1022	3.5576

$[Cu_2LCl_3(H_2O)_5]>[Zn_2LCl_3(H_2O)]>[Ni_2LCl_3(H_2O)_5]>[Co_2LCl_3(H_2O)_5]$

Non-linear optical properties

The calculated electronic properties such as dipole moment, polarisability, HOMO, LUMO energies and their energy gap are computed to examine the non-linear optical properties of the studied compounds. The Co (II) complex is found to have low energy gap between HOMO and LUMO and high dipole moment. As the lower energy gap indicates the more facile electronic transition which is the basic requirement for good linear optical properties so Co(II) complex has good optical properties. Other complex compounds have also better optical properties than the ligand.

QSAR properties

The QSAR properties of the ligand and its metal complexes are computed and given in the Table 7. The lipophilicity of the complex compounds can be predicted from the log p value and the lipophilicity of a compound is related to its biological activity. The log p value suggests the metal complexes except the Zn(II) complex are more lipophilic than the free ligand.

Table 7: Electronic properties of the ligand and its complexes

Compound	Dipole moment/Debye	Polarizability	HOMO/eV	LUMO/eV	ΔE / eV
Ligand	5.0612	22.94	-8.4928	0.5010	8.9938
$[Co_2LCl_3(H_2O)_5]$	18.018	32.85	-4.5571	-0.9954	3.5617
$[Ni_2LCl_3(H_2O)_5]$	13.11	32.84	-6.2177	-1.5588	4.6589
$[Cu_2LCl_3(H_2O)_5]$	15.016	32.83	-7.0774	-1.4484	5.6290
$[Zn_2LCl_3(H_2O)]$	12.509	29.23	-8.7610	-1.4435	7.3175

Table 8: QSAR properties of the ligand and its complexes

Compound	Log p	Polarisability	Hydration energy	Refractivity	Surface area
Ligand	-1.97	22.94	-19.46	77.24	455.50
$[Co_2LCl_3(H_2O)_5]$	-4.40	32.85	-64.16	90.93	547.96
$[Ni_2LCl_3(H_2O)_5]$	-3.38	32.84	-45.61	93.56	546.62
$[Cu_2LCl_3(H_2O)_5]$	-2.66	32.83	-63.82	90.31	598.70
$[Zn_2LCl_3(H_2O)]$	-0.89	29.23	-38.78	89.60	666.61

CONCLUSION

The first part of the work involves synthesis of the ligand and its metal complexes, their analytical study, characterisation of the studied compounds using spectral techniques such as IR, NMR and Electronic spectra. The analytical study

confirms their stochiometric composition, the spectral study indicates mode of bonding between the ligand and metal ions and geometry of the complex compounds.

The computational study of the investigating compounds is made in the second part of the study. The calculated frequency and wave length of the studied compounds are in good agreement with the experimental values. Global reactive descriptors, selected bond length and non-linear optical properties are also computed. This study indicates that complexes are more reactive than the free ligand; they complexes have also possessed more optical properties than the free ligand. The QSAR properties of the studied compounds are also presented.

REFERENCES

[1] Hallas, G. and Choi, J.H., *Dyes Pigm*, **1999**. 40: pp. 119-129.
[2] Abdel-Latif, E., et al., *Dyes Pigm*, **2009**. 38: pp. 105-110.
[3] Gratzel, M., *Nature*, **2001**. pp. 338-344.
[4] Mahmood, A., et al., *Comp Theo Chem*, **2015**. 1066: pp. 94-99.
[5] Bagihalli, G.B., et al, *Eur J Med Chem*, **2005**. 43: pp. 2639-2649.
[6] Becke, A.D., *J Chem Phys*, **1993**. 98: pp. 5648-5652.
[7] Lee, C., Yang, W.R. and Parr, G., *Phys Rev B*, **1998**. 37: pp. 785-789.
[8] Saxena, A. and Tandon, J.P., *Polyhedron,* **1984**. 3: p. 681.
[9] King, R.B., *Inorg Chem*, **1961**. 5: p. 300.
[10] Bellamy, L.J., John Wiley, 2nd edn., New York, **1964**.
[11] Stefov, V., Petrusevski, V.M. and Soptrajanov, V.M., *J Mol Struct*, **1961.** 97: p. 2939.
[12] Nakamoto, K., Wiley and sons, **2009**.
[13] Lever, A.B.P., *Coord Chem Rev*, **1968**. 3: p. 119.
[14] Shakir, M., Mahammed, A.K. and Nasman, O.S.M., *Polyhedron*, **1996**. 15: pp. 3487-3492.
[15] Yamada, S., *Coord Chem Rev*, **1966**. 1:p. 445.
[16] Lever, A.B.P. and Solomon, E.I., Wiley and sons, **2014**.
[17] Murray, J.S. and Sen, K., Elsevier, **1996**.
[18] Parr, R.J. and Pearson, R.J., *J Am Chem Soc*, **1983**. 7512: p. 105.
[19] Soliman, S.M., et al., *J Chem Sci*, **2015.** 127: pp. 2137-2149.